Site-Directed Immobilization of Bilirubin Oxidase for Electrocatalytic Oxygen Reduction

Firas Al-Lolage, Philip Bartlett, Sébastien Gounel, Priscilla Staigre, Nicolas Mano

Site-directed Immobilization of Bilirubin Oxidase for Electrocatalytic Oxygen Reduction

Firas Al-Lolage,[a,b] Philip N. Bartlett,[a*] Sébastien Gounel,[c] Priscilla Staigre[c] and Nicolas Mano[c]

[a] School of Chemistry, University of Southampton, Southampton, SO17 1BJ, UK

[b] Department of Chemistry, College of Science, University of Mosul, Mosul, 41002, Iraq

[c] CNRS, Univ. Bordeaux, Centre de Recherche Paul Pascal (CRPP), UMR 5031, 33600 Pessac, France

Abstract

In this work we extended the generic approach for the site-directed immobilization of enzymes based on maleimide\thiol coupling of engineered enzymes to the oriented immobilization of variants of bilirubin oxidase from *Magnaporthe oryzae* (*Mo*BOD) to electrodes. We show that this approach leads to the stable attachment of the enzyme to the electrode surface and that the immobilised *Mo*BOD variants are active for bioelectrocatalytic reduction of di-oxygen through direct (unmediated) electron transfer (DET) from the electrode. For the three *MoBOD* variants studied significant differences are observed in the kinetics of DET that relate to the orientation of the enzyme and the distance of the T1 site from the electrode surface. The stability of the immobilized enzymes allows us to compare the DET and mediated electron transfer (MET) pathways and to investigate the effects of pH and Cl^-. Our studies show a change in the slope of pH dependence at pH 6.0 and highlight the effect of Cl^- on the direct oxygen reduction by *Mo*BOD as a function of pH for the immobilized enzyme and the interconversion of the resting oxidized (RO) form of the immobilized enzyme and the alternative resting (AR) state formed in the presence of Cl^-.

Keywords: bilirubin oxidase, direct electron transfer, oxygen reduction, site directed mutagenesis, immobilization, maleimide

1. INTRODUCTION

Bilirubin oxidase (BOD) (EC 1.3.3.5) belongs to the multicopper oxidase (MCO) family, a large group of enzymes, including laccase, CueO, Fet3p, and BOD.[1] The MCO family is one of a few enzyme classes capable of reducing O_2 to water.[2] To date, seven BODs have been isolated,[3] among which are BOD from *Magnaporthae oryzae* (*Mo*BOD),[2] BOD from *Myrothecium verrucaria* (*Mv*BOD), BOD from *Trachyderma tsunodae* (*Tt*BOD),[4] and BOD from *Bacillus pumilus* (*Bp*BOD).[5] The two recently identified enzymes, *Mo*BOD and *Bp*BOD show a high activity at pH 7, good thermal stability and a low sensitivity toward chloride under physiological conditions. These desirable features make these BODs attractive for possible application in biofuel cells operating under physiological conditions.[6]

BODs contain four coppers classified depending on their optical and electron paramagnetic resonance properties. Their exact electronic pathway has yet to be confirmed, however it is assumed that the type one copper center (T1) receives electrons from an electron donating substrate and relays them to the O_2 reduction site through ~13 Å of Cys-His residues. The O_2 reduction site is a trinuclear cluster (TNC), composed of one type two copper ion (T2) and a pair of type three copper ions (T3).[7, 8] Only two crystal structures of BODs are available so far, those for *Mo*BOD[1] and *Mv*BOD.[3, 9] Figure 1 (left) shows the Pymol generated image of the structure of BOD, a 64-kDa protein, from *Magnaporthe oryzae* (*Mo*BOD) showing the four Cu centers. Figure 1 (right) shows the BOD active site with arrows marking electron flow from the T1 to the TNC.[10, 11]

The modification of electrodes is an effective method to improve the interfacial electron transfer to BODs. Modification has been achieved using a range of methods, including covalent modification by diazonium coupling[12] or oxidation of amines,[13] physical adsorption[14] and utilization of functionalized carbon nanotubes (CNTs).[15] However, these reported approaches do not allow precise control over the orientation and environment of the enzyme attached to the electrode surface. To address this problem several selective immobilization methods that work under mild conditions have been studied.[16] We recently described a flexible, generic approach based on the combination of site-directed mutagenesis, electrografting and solid phase synthesis methodology that provides a modular approach that allows the different components to be varied independently.[17, 18] In the present work we apply this to the immobilization of bilirubin oxidase using the coupling of maleimide groups on the electrode surface to cysteine residues introduced at specific positions on the enzyme surface. Three BOD variants have been used in this study, modified to bear a free cysteine residue in different positions at the surface of

the enzyme. This allows us to investigate the effects of enzyme orientation on the electrocatalytic reduction of oxygen. In addition, because of the excellent stability of the immobilized enzyme, we are able to investigate the effects of pH and Cl^- on the catalytic process.

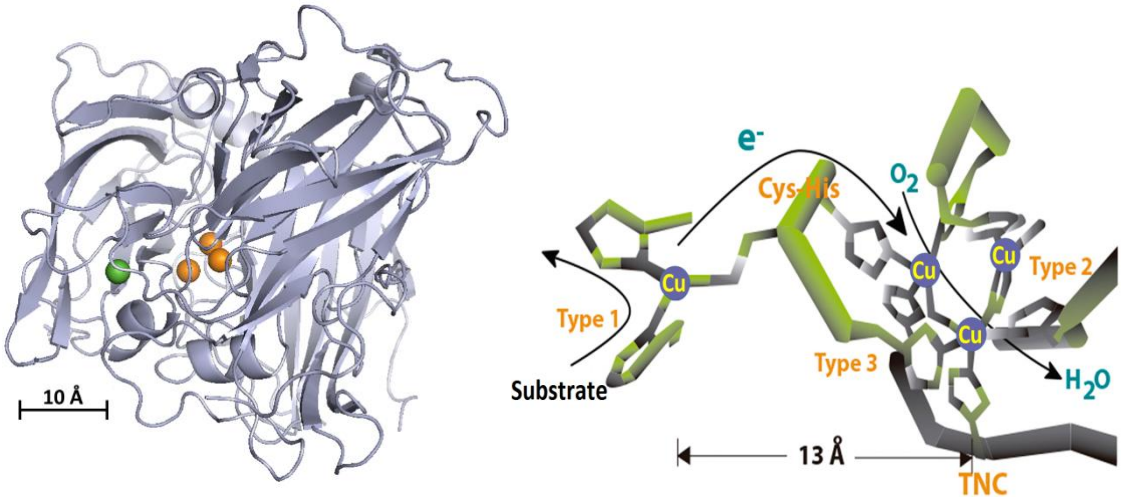

Figure 1. Left) Cartoon representation of the secondary structure of bilirubin oxidase from *Magnaporthe oryzae*. The Type 2 and Type 3 (TNC) coppers are represented by orange spheres, the Type 1 Cu is represented by the green sphere. The image was obtained with PyMol software, PyMol visualisations are based on the crystal structure of *Mo*BOD, PDB code 2L9Y.[7] Right) Structure of the BOD active site with arrows marking flow of substrate, electron (e^-) from the T1 to the TNC, and O_2. (Adapted with permission from reference 11. Copyright 2015, PLOS One under CC BY 4.0

2. METHODS

2.1 Chemicals and Materials. All chemicals were of analytical grade and used without further purification unless otherwise stated; aqueous solutions were prepared using deionized Millipore-Q water (18.2 MΩ cm) from either a Purite or AQ 10 Milli-Q system. Argon (Pureshield, 99.998%) and oxygen were supplied by BOC gasses, ABTS (2,2'-azino-bis-[3-ethylbenzthiazoline-6-sulfonic acid]) was obtained from Fluka.

Multi-walled carbon nanotube (MWCNT) working electrodes were prepared as described in our previous work.[17] Briefly, 5 µL of a DMF dispersion of 1 mg cm^{-3} of carbon nanotubes (Aldrich, > 8% carboxylic acid functionalized, average diameter and length 9.5 nm and 1.5 µm)

were placed onto a 3 mm diameter glassy carbon (GC) surface (SIGRADUR HTW Hochtemperatur – Werkstoffe GmbH, Germany) using a plastic mask to control the spread of the dispersion, and then left to dry at ambient temperature for 2 days. To ensure reproducibility the glassy carbon was first polished using silicon carbide (grade 1200 paper) and alumina (1.0 and 0.3 μm, Buehler) followed by sonication in deionized water and ethanol. This method gives a reasonably uniform coating of MWCNTs across the electrode surface with a total surface area of around 12 cm^2 and good (+/- 10%) reproducibility and stability. [17, 19]

A standard three electrode arrangement was used with either a homemade saturated calomel (SCE) or saturated mercurous sulfate (SMSE) reference electrode and large area Pt gauze counter electrode. Either a μAutolab type III or an Autolab PGSTAT 302 (Ecochemie, Netherlands) was used.

2.2. Modification of GC/MWCNT electrodes with maleimide. The modification of the multiwalled carbon nanotube electrodes followed the procedure described previously[17] and summarized in Figure 2. The nanotubes were modified by electrografting from a TBATFB (0.1 M) acetonitrile (HPLC grade, Fisher Scientific) solution containing a mixture of two primary amines; N-Boc-1,6-hexanediamine (2 mM, Sigma Aldrich) and N-(2-aminoethyl) acetamide (18 mM, Sigma Aldrich). The electrografting was carried out in deoxygenated solution by potentiostatic oxidation of the amines at +2 V *vs*. SCE for 180 s. After attachment of the amines the electrode was washed (acetonitrile) and then the BOC protecting group removed by gently stirring for 45 min in 4 M HCl in dioxane (Certified ACS grade, Fisher Scientific). In the next step a 6 carbon-spacer was coupled to the free amine by placing the electrode for 16 h in a DMF solution of N-Boc-6-aminohexanoic acid (10 mM, Sigma Aldrich), N-(3-dimethylaminopropyl)-N′-ethylcarbodiimide (EDC, 0.1 M, Sigma Aldrich) and N-hydroxysuccinimide (NHS, 60 mM, Sigma Aldrich). After coupling, the electrode was washed (acetonitrile then water) and dried before again removing the BOC protecting group as before (gently stirring in 4 M HCl/dioxane for 45 min). In the final step the maleimide was coupled to the free amine using N-maleoyl-β-alanine (25 mM, Sigma Aldrich), NHS (60 mM) and EDC (0.1 M) in DMF by immersion for 16 h followed by washing (acetonitrile then water) and drying.

2.3. *Mo*BOD variants. pPicZα vector and *E. coli* DH5α and *P. pastoris* GS115 strains were obtained from Invitrogen. LB (Luria-Bertani) medium, YPD (yeast extract dextrose) medium and MMH (Minimal Methanol Histidine) were prepared following the Pichia Expression Kit (Invitrogen). AKTA purifier10 UV-900, prepacked HiLoad 26/10 Phenyl Sepharose HP (53

mL) columns were obtained from GE Healthcare Bio-Sciences AB (Uppsala, Sweden), Amicon Ultra ultrafiltration columns were from Millipore (Molsheim, France). VivaFlow 200 cassettes were purchased from Sartorius. UV–visible measurements were carried out using a Cary 100 system (Varian) fitted with a Peltier thermostable multicell holder. Polymerase chain reactions were carried out in a VWR automated thermal cycler. An Eppendorf electroporator was used to introduce DNA into *E. coli* and *P. pastoris* GS115.

The construction vector for the WT production was previously described.[5] Briefly the open reading frame of the BOD (Genbank accession EDJ95889.1) from *M. oryzae*, deleted from its first 24 amino acids, was introduced in a pPicZα in NheI and NotI. A QuickChange site-directed mutagenesis kit was used for the mutations. For each mutant, two primers were designed for PCR-based site-directed mutagenesis to create the BOD Cys mutants.

A164C : Froward : ccccgccgaggactgcctcaacctcccc

Reverse : ggggaggttgaggcagtcctcggcgggg

S362C : Forward : ccaccgccaaaagtgcgagtggcgcatc

Reverse : gatgcgccactcgcacttttggcggtgg

N375C : Forward : cctttgccgacgtctgcaaccgcatgctcgcc

Reverse : ggcgagcatgcggttgcagacgtcggcaaagg

The presence of mutations was verified by DNA sequencing after amplification of the DH5α and the extraction of the plasmid with the Qiaprep spin Miniprep Kit. The pPicZα-mutant was then linearized and transfected in *P. pastoris* GS115 strain. Positive clone was selected on YPD-agar plate with 600 µg/mL zeocin (Invitrogen). A positive clone was cultivated overnight in 50 mL YPD with 100 µg/ml zeocin overnight at 30 °C and 190 rpm. 5mL of culture was used to inoculate 2 L of MMH medium with 5 g/l glycerol in a 5 L flask and cultivated 48 h at 30°C and 190 rpm. After 48 h, 0.15 mM $CuSO_4$ was added to the culture and the temperature was set at 25 °C. The protein induction was performed with 0.5 % of methanol (v/v) and was repeated daily for 3 days. The culture was finally centrifuged at 6000 g for 20 min at 4 °C to remove yeast cells.

The culture supernatant was then filtered (0.5 µm) and concentrated to 100 mL with a VivaFlow 200 30 kDa before purification. The BODs were purified as previously described.[5]

2.4. Enzyme assay. The BOD activity was measured at 37 °C in pH 4 citrate–phosphate buffer (McIlvaine) using the oxidation of 4 mM ABTS at 420 nm (ε 420 nm 36 mM^{-1} cm^{-1}). One unit is defined as the amount of enzyme that oxidizes 1 mol of substrate in 1 min. The activities were 564±30 U/mg for A164C, 516 ± 38 U/mg for S362C and 375 ± 48 U/mg for N375C. Activities were also measured in a 100 mM pH 7 phosphate buffer with 90 µM syringaldazine (ε_{530nm} = 64 $mM^{-1}cm^{-1}$), they were: 8 ± 1 U/mg for the WT, 7.0 ± 0.6 U/mg for A164C, 7.0 ± 0.5 U/mg for S362C and 6.2 ± 0.8 U/mg for N375C. The BOD variants were stored in 25 mM sodium phosphate buffer (pH 6.0) at -80 °C. The storage buffer was exchanged for 50 mM, pH 7.0, phosphate buffer using mini dialysis devices with a PES membrane (10 kDa cut off, Fisher Scientific). After dialysis, 3 µL of the solution of the selected BOD variant was placed on the maleimide modified electrode and left overnight to react at 4 °C.

2.5. Oxygen reduction. Measurements of the oxygen reduction currents were made in 200 mM phosphate, 100 mM citrate (McIlvaine) buffer solution, pH 7.0. Solutions were sparged with oxygen for 8 min before measurement to ensure saturation.

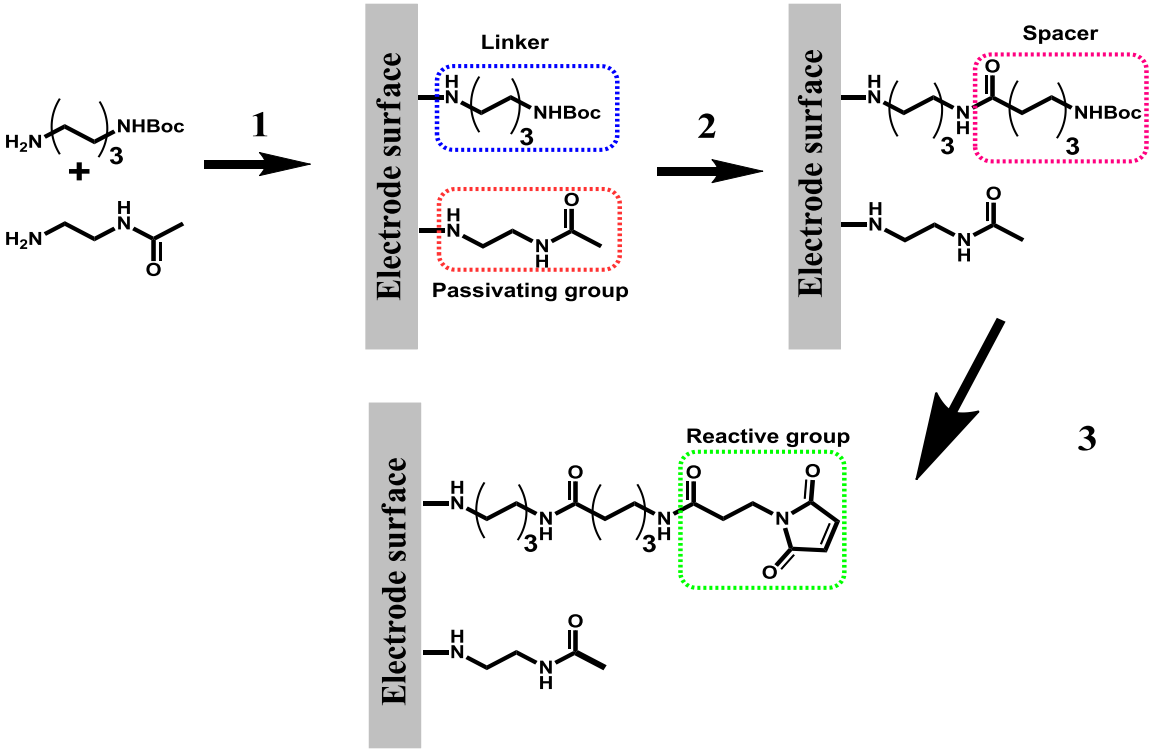

Figure 2. Sequential electrochemical and solid-phase preparation of maleimide-modified working electrodes. 1) Attachment of linker and capping group at the electrode surface via electrochemical oxidation of N-Boc-1,6-hexanediamine and N-(2-aminoethyl)acetamide in acetonitrile containing TBATFB, applying a constant potential of 2 V *vs*. SCE for 180 s. 2) Boc-deprotection of the linker in 4 M HCl in dioxane (45 min), followed by EDC/NHS coupling of 6C- spacer in DMF (16 h). 3) Boc-deprotection of the spacer in 4 M HCl in dioxane (45 min), followed by EDC/NHS coupling of maleimide group in DMF (16 h).

3. RESULTS AND DISCUSSION

Three genetically engineered *Mo*BOD variants, S362C, A164C and N375C have been used in this study. They were modified to bear a free single cysteine residue in different positions on the enzyme surface (there are no –SH residues on the surface of the wild type enzyme) allowing site-specific attachment to the maleimide-modified electrodes, Figure 3. The distances between the T1 site and the cysteine modification are: S362C 1.33 nm, N375C 2.29, nm and A169C 3.98 nm.

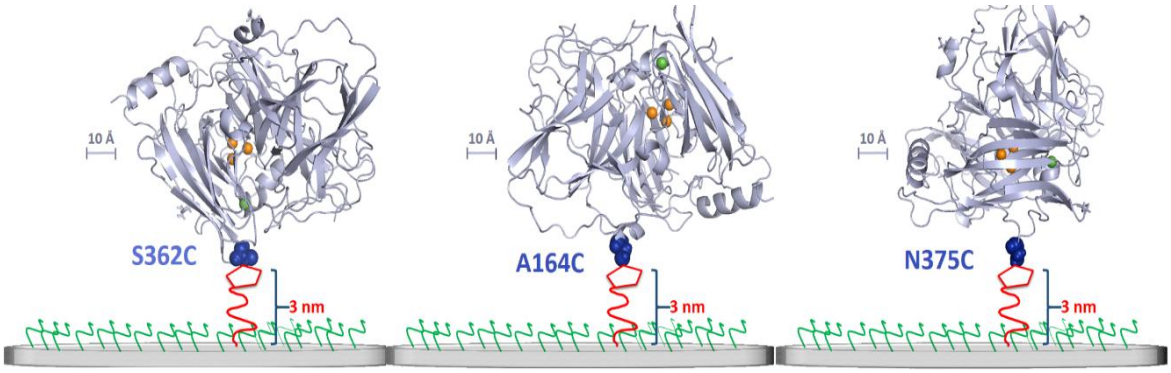

Figure 3. Cartoon representation showing the secondary structure of the three *Mo*BOD variants and their attachment to the maleimide modified surface. The location of the engineered cysteine residue on the surface is highlighted in blue. (PyMol visualisations are based on the crystal structure of *Mo*BOD, PDB code 2L9Y.[7])

Multiwall carbon nanotube modified glassy carbon electrodes (GC/MWCNT) were used because they give a high surface area combined with a relatively low capacitance. These were modified with maleimide groups following a modular approach combining electrochemical

surface attachment and solid phase synthesis methodology.[17, 18] This provides a diluted coverage of maleimide groups on the surface, allows control over the length of the linker and allows the surrounding surface to be passivated by modification with other groups chosen to be compatible with the enzyme. In this case a 10 % coverage of maleimide was chosen with a 6-carbon spacer together with acetamide passivating groups (Figures 2 and 3) based on our earlier work with cellobiose dehydrogenase.[17] The coverage was controlled by choice of the relative concentrations of the two primary amines.[20] Note that the tether has a total length of ~3 nm but is flexible so that the distance for electron transfer will be less than this. The use of the maleimide group allows specific coupling to the free thiol of the surface cysteine at pH 7 without the need of added reagents providing a very flexible approach to the stable, orientated immobilization of enzymes at electrode surfaces.

3.1. Direct electron transfer at BOD-modified electrodes. GC/MWCNT electrodes modified with the BOD-S362C variant were tested for direct electron transfer (DET) and mediated electron transfer (MET) by cyclic voltammetry in pH 7.0 phosphate-citrate buffer solution. Figure 4 shows results for DET (black and green curves) and MET with 2, 2'-azino-bis(3-ethylbenzothiazoline-6-sulphonic acid) (ABTS) as the solution mediator (blue and red curves). Considering the DET first, in oxygen saturated solution (Figure 4A green line) the current onset starts at around 0.46 V *vs.* SCE and reaches a plateau at about 0.3 V *vs.* SCE. The position of the electro-catalytic wave agrees with that reported in the literature for adsorbed BOD at carbon nanofiber,[10] gold nanoparticle,[21] and carbon nanotube[22] electrodes. Note that the first voltammetric cycles in the presence of oxygen differ from the second and subsequent cycles (a point we return to below) and so, unless otherwise stated, the second cycles are shown.

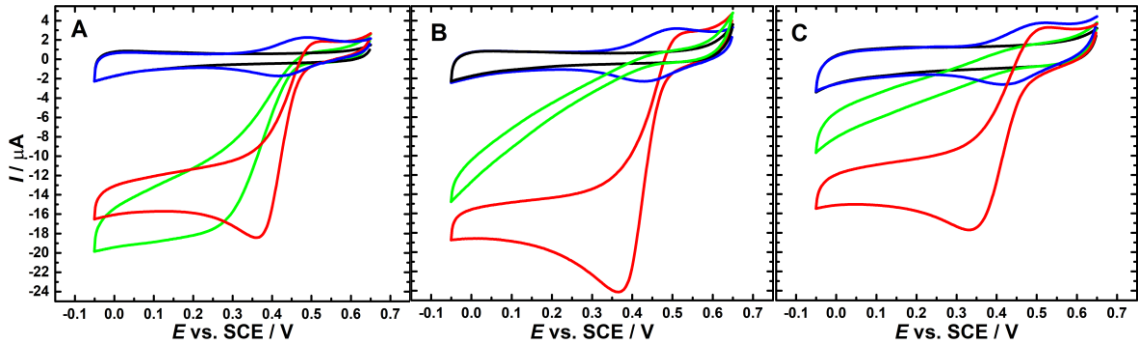

Figure 4. Comparison of the results for DET and MET. The black and green curves show DET in deoxygenated and oxygen–saturated solutions. The blue and red curves show MET in deoxygenated and oxygen–saturated solutions containing 0.3 mM ABTS for the same electrodes. In each case the second scan is shown. A) Electrode with BOD variant S362C immobilized by covalent attachment through maleimide. B) Control electrode prepared using maleimide-modified GC/MWCNT electrode and wild type *Mo*BOD made by drop casting 3 μL of the enzyme solution on the electrode. C) Control electrode prepared using bare GC/MWCNT electrode and the S362C BOD variant made by drop casting 3 μL of the enzyme solution on the electrode. Voltammograms recorded at 10 mV s^{-1} in pH 7.0 phosphate-citrate buffer.

To verify that the BOD variant was immobilized at the electrode surface through covalent bonding through the surface cysteine, we carried out two control experiments: using the maleimide modified electrode with the wild type *Mo*BOD that has no surface cysteine residues (Figure 4B), and using an unmodified GC/MWCNT electrodes with the S362C *Mo*BOD variant (Figure 4C). In both these cases non-specific adsorption of the enzyme can occur but not site specific covalent linkage. The DET voltammetry in oxygen free solution (black curves) shows very similar background capacitance for the two maleimide modified electrodes (Figure 4A and B) but slightly larger capacitance for the bare GC/MWCNT electrode (Figure 4C). This reflects the effect of the covalently attached maleimide and acetamide groups on the MWCNT surface.

In oxygen saturated buffer solution the electrode with the covalently attached S362C variant and the two control electrodes show clearly different responses. Although direct electron transfer and catalytic reduction of oxygen is observed in all three cases (Figure 4 green curves) the responses for the two control electrodes (Figure 4B and C) are lower, more drawn out with potential, and do not reach a plateau. Clearly the non-specifically adsorbed enzyme is able to undergo DET but this is not as effective as for the covalently linked enzyme under these conditions. For the MWCNTs used we expect the surface to be negatively charged at pH 7[23] and this can affect to possible orientation(s) of the adsorbed enzyme.[24, 25] The drawn out shape of the voltammograms for the adsorbed enzyme can be explained in terms of disorder among the immobilised enzyme molecules participating in DET resulting in a spread of electron transfer rates reflected by the trailing edge in the catalytic cyclic voltammogram.[26] Similar behavior has been observed for several multi-centered redox enzymes[27-30] and even for simpler systems such as cytochrome *c* peroxidase.[31] Thus, the results in Figure 4 are consistent with covalent binding

of the cysteine-modified *Mo*BOD at the maleimide-modified electrodes in a well-defined orientation and much faster DET to the covalently bound S362C variant.

To exclude the possibility that the differences in the catalytic currents might be due to significant differences in the enzyme loadings on the different electrodes we used ABTS as a mediator.[32] This solution mediator should be able to react with all of the enzyme molecules on the surface of the electrode.[33] The same three electrodes were re-tested by monitoring the catalytic current caused by MET in the presence of 0.3 mM ABTS as a mediator (Figure 4 blue and red curves). Note that the increasing the ABTS concentration to 0.75 mM had no significant effect on the catalytic current indicating that mass transport of mediator was not rate limiting.

Looking at the results in the oxygen free solution (Figure 4, blue curves) we can see the ABTS voltammetry at around 0.45 *vs*. SCE. In oxygen saturated solution in each case (red curves) there is a clear catalytic wave around 0.45 V rising to a plateau at more negative potentials. Comparing the results in Figure 4A for the direct and ABTS mediated oxygen reduction at the electrode with the covalently bound *Mo*BOD variant S362C we can see that the ABTS has little effect on the limiting catalytic current indicating that the DET was not rate limiting at negative potentials. In contrast for the two control electrodes it is clear that the mediated electron transfer through the ABTS is more effective that the direct electron transfer in both cases (compare Figures 4B and 4C).

To further confirm the covalent immobilization of the S362C variant on the maleimide modified electrode surface the stability over time of the electrode was compared with that for the physically adsorbed wild-type BOD on the maleimide-modified GC/MWCNT electrode. The electrodes were tested in oxygen saturated buffer at regular intervals and stored in a deoxygenated wet condition at 4 °C between measurements. Figure 5 shows that the covalent immobilized enzyme (black curve) shows better stability than the control (red curve) with around 95% of the initial response retained after 3 days storage and around 48% retained after 6 days. Previous work on engineered cellobiose dehydrogenase immobilised through the thiol/maleimide linkage on the same type of electrodes has shown stability for over 1 month[17] so we do not believe that the decrease seen for the immobilized S362C BOD variant can be attributed to loss of MWCNT from the electrode surface or to cleavage of the thiol/maleimide linkage. We speculate that in the present case the slow decay of activity is due denaturation of the enzyme and/or loss of copper from the enzyme-active site; this speculation is consistent with the findings of several published studies on BOD modified electrodes.[34-36]

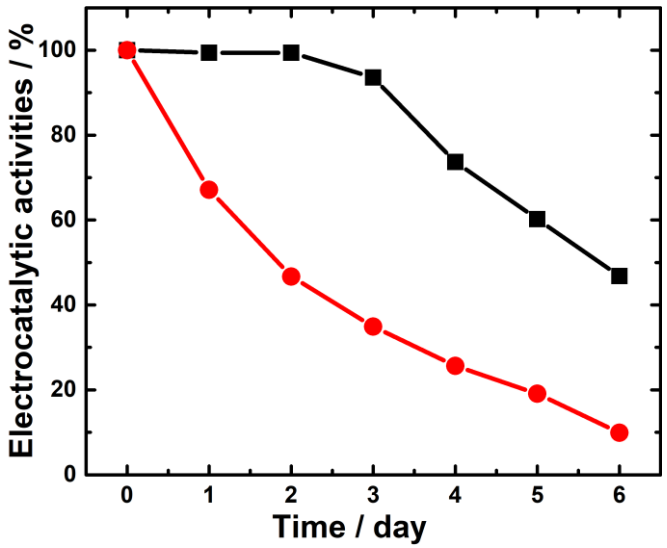

Figure 5. The maximum electrocatalytic activities of the maleimide modified GC/MWCNT electrodes covalently modified with S362C-BOD variant (black line) and adsorbed WT-BOD (red line) as a function of the length of storage. Electrocatalytic currents were measured in oxygen-saturated pH 7.0 phosphate-citrate buffer at 0.0 V *vs*. SCE.

3.2. The effect of enzyme orientation. Two further BOD variants (see Figure 3 for the structures) with a cysteine residue introduced at a different location on the protein surface were investigated to study the effect of the orientation of the enzyme on the surface. The three different variants, S362C, A164C and N375C place the T1 copper site of the enzyme at different distances (S362C closest, A164C furthest) from the electrode surface. The three variants were immobilized onto maleimide modified GC/MWNT electrodes as before. Figure 6 shows voltammetry for the three electrodes in pH 7.0 buffer in the oxygen-saturated solution for both DET (green curves) and for mediated electron transfer with ABTS (red curves). Note that these results were reproduced on at least two replicate electrodes for each variant. All three variants show bioelectrocatalytic activity towards oxygen reduction in both DET and MET starting at onset potentials of around 0.46 V *vs*. SCE. For the A164C and N375C variants the DET current does not reach a plateau (Figure 6B and C, green curves) indicating that interfacial electron transfer was slower[3, 37] than for the S362C variant.

Comparing the results for mediated electron transfer at the three electrodes (Figure 6, red curves) the currents for the S362C and A164C variants are very similar, indicative of similar loadings for the two variants. Thus we can conclude that the fast direct electron transfer achieved for the S362C variant is due to a more favourable orientation of this variant on the

surface of the electrode rather than due to higher enzyme surface coverage. This can be attributed to the different orientation of the BOD variant on the electrode surface that places the T1 site closer to the electrode surface (Figure 3). The MET current for the N375C variant is notably smaller (Figure 6C) and this result was confirmed in replicate measurements and using different preparations of the N375C. It can be explained by the lower activity of this mutant due to the mutation and/or by some hindrance in coupling to the cysteine residue at this position.

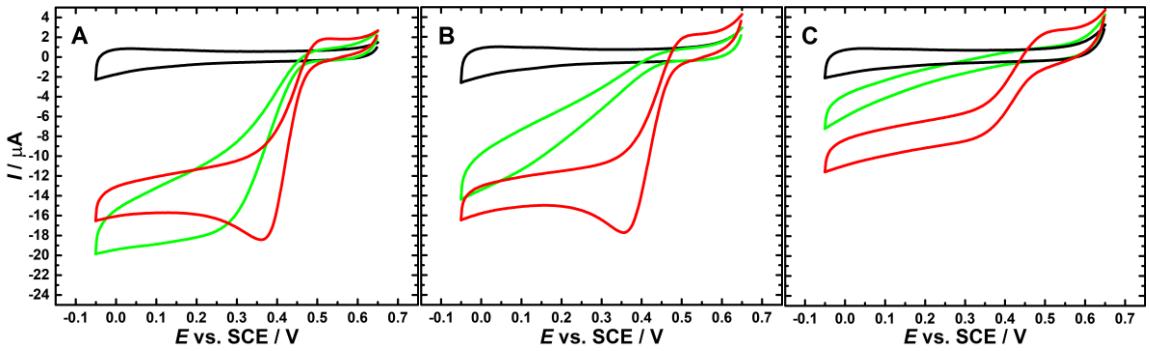

Figure 6. Typical cyclic voltammograms showing the response of GC/MWCNT electrodes for various covalently immobilized variants: (A) S362C, (B) A164C and (C) N375C to ORR in oxygen-saturated (red) and deoxygenated (black) pH 7.0 phosphate-citrate buffer solution, and after the addition of 0.3 mM ABTS (red), scan rate of 10 mV s^{-1}. In each case the second scan is shown. The GC/MWCNT electrodes were prepared by drop casting of 5 µL of 1 mg mL^{-1} MWCNT dispersion onto the cleaned surface of GC. The *Mo*BOD variants were immobilised at the electrode surfaces via the thioether bond.

3.3. Effect of solution pH. It is widely believed that the cathodic current onset at around 0.46 V *vs.* SCE at pH 7 (see Figure 4) corresponds to the BOD-T1 site.[38-41] Indeed, it has been difficult to obtain electrochemical evidence for BOD electroactivity at lower potentials. However, some authors have tried to assign peaks in the range 300–500 mV *vs*. Ag/AgCl to the BOD-T3 site[38, 42, 43] and peaks in the range 100–300 mV *vs*. Ag/AgCl to the BOD-T2 site.[39, 43]

In this study we investigated the pH dependence of the DET oxygen reduction for the immobilized S362C variant over the range pH 4.0 to 7.6 (Figure 7A). Whilst the limiting current for oxygen reduction remains practically constant at about 16 µA the onset potential for O_2 reduction clearly shifts with pH (Figure 7B). Between pH 6 and 7.6 (using a universal buffer system, phosphate (200 mM)-citrate (100 mM) (McIlvaine) buffer) the onset potential shifts by

about -57 mV for each unit change in pH corresponding to a $1e^-/1H^+$ process. In the region between pH 4 and pH 6 the shift is less, about -28 mV for each unit change in pH. Similar, sub-Nernstian responses have been reported for T1 Cu sites in other multicopper oxidases[3, 44, 45] and are probably due to the involvement of protonation/deprotonation of amino acid residues in the neighbourhood of the T1 site.

In a recent study Filip and Tkac[46] observed a decrease of the redox potential for the T1 site with pH with a slope of -66 mV/pH in two different buffer systems (acetate and HEPES) for pH between 5.0 and 7.5. . In another study Weigel *et al.*[47] reported a slope of -54.5 mV/pH for the dependence of the T1 site in BOD over the range pH 4.0 to 8.0 in citrate-phosphate buffer. However, Shleev *et al.*[45] reported a variation of the BOD-T1 site potential with pH of -23 mV/pH in a universal buffer (phosphoric, boric and acetic acids) for pH between 4.2 and 7.0. These differences could be due to the different enzyme immobilization methods and/or the different buffers used for the measurements.[46]

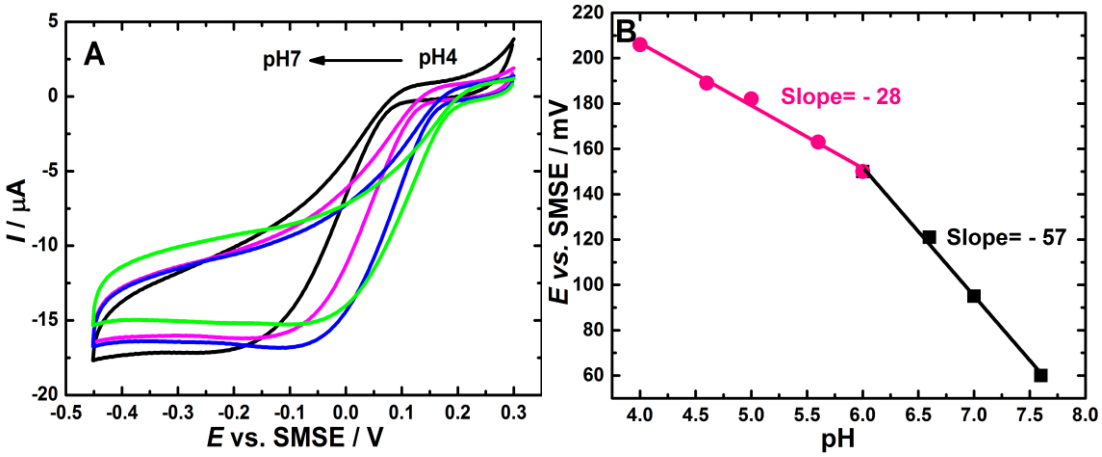

Figure 7. (A) Cyclic voltammograms of S362C at maleimide-modified GC/MWCNT electrode in various oxygenated solutions (pH 4.0, 5.0, 6.0, and 7) at 10 mV s^{-1}. In each case the second scan is shown. Measurements were performed in universal buffer system (200 mM phosphate, 100 mM citrate (McIlvaine buffer). Note potentials are with respect to SMSE to avoid contamination by Cl^- (see text). (B) The onset potential of reduction of O_2 plotted vs. pH.

The clear break in the pH dependence of the onset potential seen at pH 6.0 in Figure 7B indicates a change in the protonation state of the species involved in the redox process. The pH dependence seen here is consistent with published studies of other copper enzymes, such as azurin[46, 48] or CueO[49] but, to the best of our knowledge, there are very few studies of the effect

of the amino acids involved in proton-coupled electron transfer in electrochemical studies of BODs.

In a recent study Cosnier *et al.*[32] suggested that a pK_{ox} of 6.0 (where K_{ox} is the proton dissociation constant for the oxidized form of BOD-T1 copper) is related to the protonation of an amino acid, such as histidine (His) in the vicinity of the BOD-T1 copper center (see Figure 8), which effects structural rearrangement of the copper during the redox process. In addition, there is agreement that two acidic amino acids, namely, glutamic acid (Glu) and aspartic acid (Asp),[46] both highly conserved amongst all MCOs,[50-53] are crucial for the enzymatic activity with participation in proton transfer during catalysis. For *Mo*BOD as used here, Glu/464 and Asp/107 are present in close proximity to the trinuclear cluster (TNC), Figure 8. In their work Filip and Tkac[46] suggested that the Asp identified in the exit channel of *Mv*BOD-TNC is involved in the reductive separation of the oxygen-oxygen bond at acidic pH, in supporting protonation of the hydroxyl groups bound to the BOD-T2 copper ion, or in governing protonation of a Glu residue and in the activation of the proton of the BOD-T2 bound water at high pH. However, Glu located in the O_2 entrance channel of the *Mv*BOD-TNC was shown to be involved in a proton transfer to the peroxide during the reductive separation of the oxygen-oxygen bond at around pH 7.[50, 54] Hence, the break point observed at pH 6 (Figure 7B) could be attributed to the protonation of the His/463 in the vicinity of the T1 copper or the Glu/463 or Asp/107 residues; although in the latter case it is not clear how amino acids identified in the BOD-TNC influences the BOD-T1 electrochemistry even though it is known that the T1 site is firmly interconnected in terms of electrochemical disruption to the BOD-TNC.[46, 55]

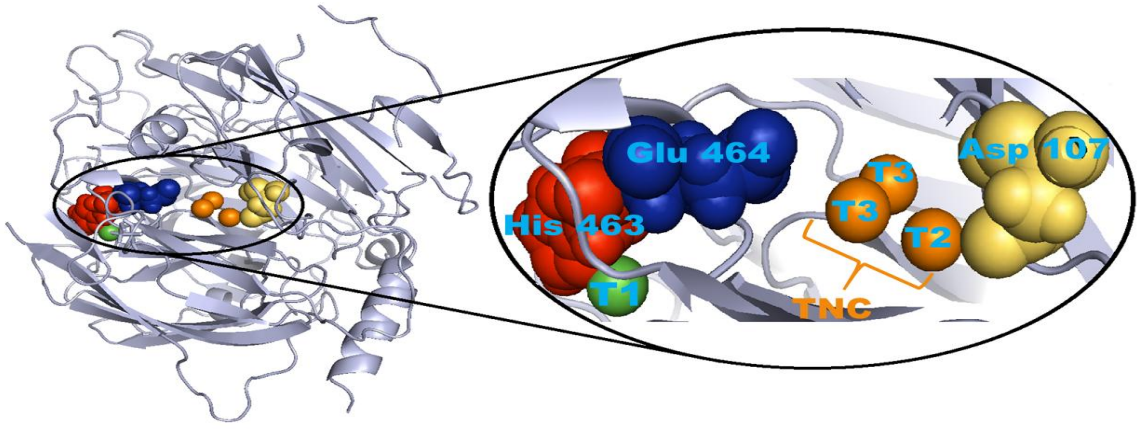

Figure 8. A schematic representation of BOD with the Cu active sites and positions of Asp 107, Glu 464 and His 463 amino acids in the enzyme shown. The BOD structure was rendered with PyMol software, PyMol visualisations are based on the crystal structure of *Mo*BOD, PDB code 2L9Y.[7]

3.4. The effect of chloride. The study of the pH dependence discussed above was initially carried out using an SCE reference electrode. However, unusual behavior was observed in the voltammetery at pH 4 that was traced to chloride contamination from the reference electrode.These effects disappeared when the reference electrode was changed to SMSE. The effects of pH and chloride ions on the BOD activity are of great importance, particularly for the application of BOD-based bio-cathodes operating in physiological conditions,[6] yet, apart from a very recent contribution,[10] there has not been a detailed study undertaken to understand the related effect of Cl^- and pH on the electrochemistry of immobilized BODs.

The influence of chloride concentration on the electrocatalytic activity of the covalently immobilised S362C variant was investigated. Figure 9 shows the results for electrocatalytic oxygen reduction at pH 4, 6 and 7 at different concentrations of chloride. It is clear that the inhibition by Cl^- is more pronounced at lower pH suggesting that it could be related to the amino acid residue protonation below pH 6.0 discussed above. At pH 4, before the addition of NaCl, the onset for O_2 reduction is observed at 0.6 V *vs*. SCE (Figure 9A, black curve) and a sigmoidal wave, typical of the catalytic reduction of O_2, is observed. Upon addition of 1.5, 5, and 10 mM NaCl to the solution, a progressive decrease in the catalytic current occurs. Furthermore, on the forward scan, the onset for O_2 reduction shifts by -50, -100, and -120 mV respectively. However the reverse scan is less influenced by NaCl, suggesting that O_2 reduction is more efficient after the enzyme has been exposed to reducing potentials.

This unusual CV shape indicates an inactivation/reactivation of BOD for O_2 reduction similar to the behavior observed with the thermostable BOD from *Bacillus pumilus* adsorbed on a graphite electrode modified with CNFs.[10] Taking into account that both Cl^- and OH^- bind to the T2/T3 TNC Cu cluster and obstruct electron transfer from the T1 site to the TNC without affecting the ability of TNC to bind O_2,[56] it can be concluded that the inhibition by chloride is due to the formation of an alternative resting form of the enzyme.

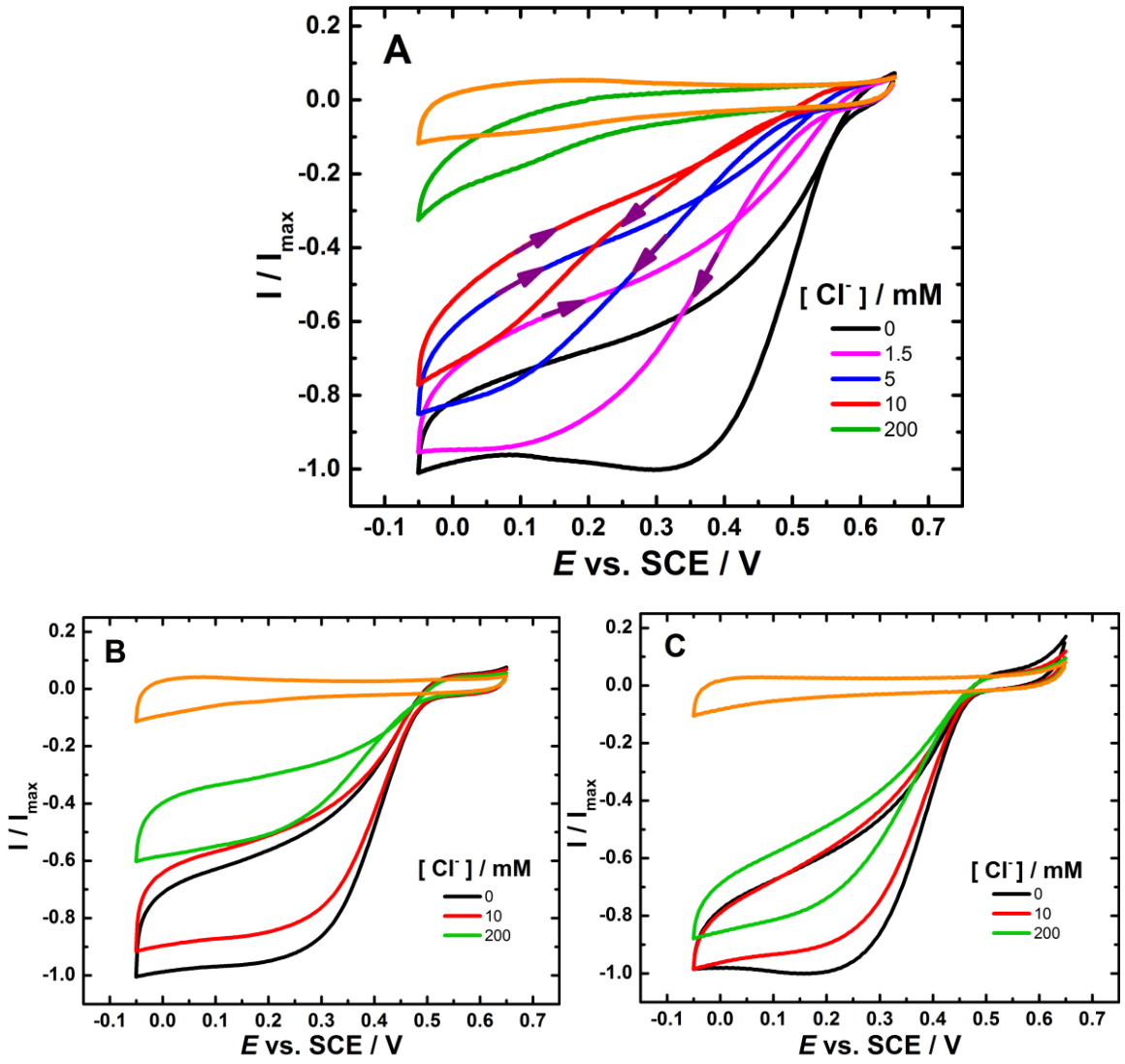

Figure 9. Voltammograms showing the response of GC/MWCNT/S632C-BOD electrode for oxygen reduction in oxygen saturated phosphate-citrate buffer solution (A) pH 4 (B) pH 6 and (C) pH 7 (black lines) and after the addition of different Cl^- concentrations (coloured lines), scan rate 10 mV s^{-1}. In each case the second scan is shown. The GC/MWCNT electrode was prepared by drop casting of 5 µL of 1 mg mL^{-1} MWCNT dispersion onto the cleaned surface of GC. The S362C-BOD was immobilized on the GC / CNT electrode using covalent attachment.

A number of investigations[1, 3, 10, 57] have explored the precise details of the electron transfer steps in BOD. Starting from the fully reduced state, reduction of O_2 occurs at the TNC, T2/T3 copper center, in two, sequential two-electron steps, where the first two-electron step produces the peroxide intermediate (PI). In the second two-electron step, the O-O bond is rapidly cleaved leading to the formation of water leaving the enzyme in the native intermediate (NI) state.[58] A sequence of steps of oxidation of substrate at the T1 site and four sequential

transfers of electrons to the TNC then completes the catalytic cycle[10], Figure 10. In the absence of substrate the NI state slowly transforms into a resting oxidized state (RO).

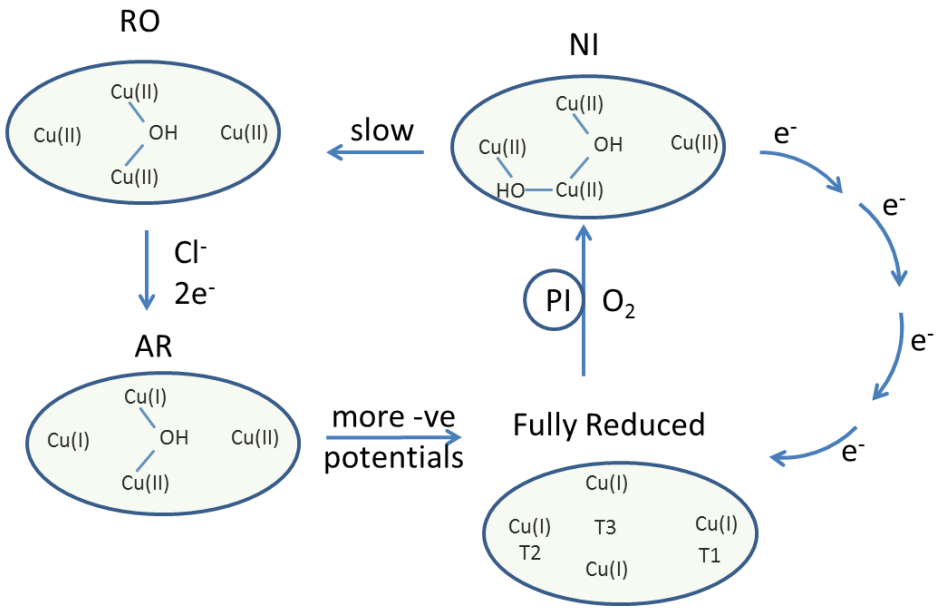

Figure 10. The *Mo*BOD catalytic cycle showing the relationship between the different states of the immobilized enzyme. The transformation of NI to RO is slow on the voltammetric timescale.

Spectroscopic characterization, supported by crystallographic data, suggests that for *Mo*BOD there are two, distinct, inter-convertible resting forms: the RO form and the AR form, detected in the as-isolated enzyme and upon Cl^- addition to the RO form.[1, 5, 11] For this alternative resting (AR) state it has been demonstrated that the TNC is partially reduced whereas in the RO state all three TNC Cu sites are oxidized.[57] Thus, once the immobilized enzyme enters the AR resting state it cannot re-enter the catalytic cycle until it is fully reduced at more negative potentials and the existence of these resting states shows up in differences between the first and subsequent potential cycles. This is consistent with the observation of Kjaergaard *et al.*[1] of a lower potential TNC Cu which needs to be reduced in the AR before the enzyme rejoins the catalytic cycle, whereas the RO form is re-activated at the higher potential of the T1 Cu.

Figure 11 shows the response of an S362C-BOD modified GC/MWCNT in oxygenated pH 7.0 phosphate-citrate buffer. The voltammetry on the first scan (black) and second (red) scans are different, with onset of catalytic current at around 425 mV *vs.* SCE on the first scan, shifting to 470 mV on the second scan. This is consistent with the existence of the two resting forms,

RO and AR, where the AR form present on the first scan (black curve) needs a be reduced at a low potential in order to rejoin the catalytic cycle and to be active for O_2 reduction whereas the RO form present on the second scan (red curve) is catalytically active from the start. Thus the peculiar CV shape in the presence of chloride (Figure 9A) and the reactivation process at low potential (Figure 11), may be attributed to the coexistence of the two resting forms of the enzyme, RO and partially oxidized AR, as previously identified for *Mo*BOD.[1]

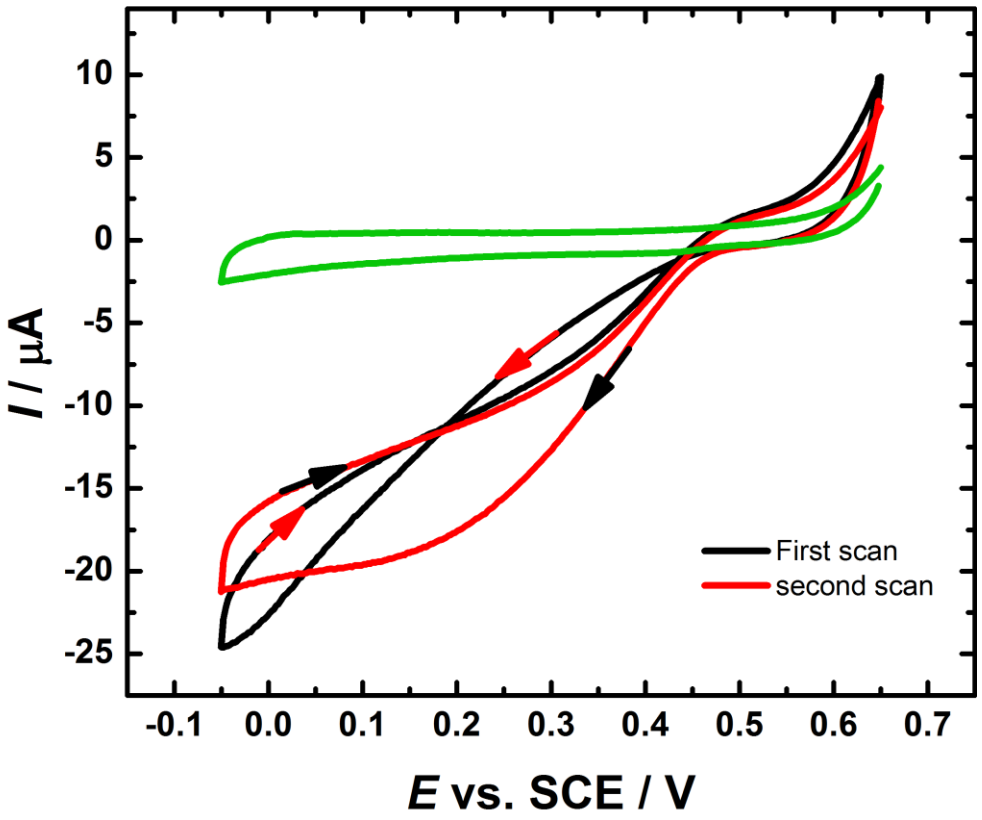

Figure 11. Typical cyclic voltammograms showing the response of a GC/MWCNT/BOD electrode to ORR in deoxygenated (green line) and oxygenated 200 to100 mM phosphate-citrate (McIlvaine) buffer solution, pH 7.0, first scan (black line), second scan (red line)at 10 mV s^{-1}. The S362C- BOD was immobilized on the GC/MWCNT electrode using covalent attachment. The experiment was conducted in the absence of Cl^- using an SMSE as reference. The potentials have been converted to the SCE scale for ease of comparison.

Returning to Figure 9, at pH 6 and 7 (Figure 9B and C) the *Mo*BOD remains in its oxidized resting state even after addition of Cl^- on the timescale of the experiment so we do not see such a marked effect. Similar results have recently been reported for *Bacillus pumilus* BOD by Lojou *et al.*[10] as a first indication that the inter-conversion between the two resting forms generated by addition of NaCl is pH-dependent. Indeed, RO/AR reciprocal conversion is not particular or

unique to *Mo*BOD. It is a common feature of BODs as well as other MCOs containing four coppers. For instance the same effect has been reported of laccase from *Bacillus subtilis*[10] and *Myrothecium verrucaria*.[11]

4. CONCLUSIONS

In this work we have extended the generic approach for the site-directed immobilization of enzymes based on the modular modification of the electrode using electrografting of amines and solid phase synthesis methodology together with the coupling of cysteine residues, introduced at the enzyme surface using site directed mutagenesis, to maleimide groups at the electrode surface. We have shown that this approach leads to the stable attachment of bilirubin oxidase from *Magnaporthe oryzae* (*Mo*BOD) to the electrode surface and that the immobilised *Mo*BOD is active for bioelectrocatalytic reduction of di-oxygen through direct (unmediated) electron transfer from the electrode.

Three different *MoBOD* variants were studied where the site of mutation was chosen to allow immobilization of the enzyme in three different orientations. Significant differences are observed for the three variants with the S362C variant in which the enzyme is oriented with the T1 Cu site closest to the electrode surface giving the fastest direct electron transfer. In contrast, for the A164C variant, in which the enzyme is oriented with the T1 site away from the electrode, the kinetics of DET were much slower leading to a drawn out catalytic current that only slowly increases with increasing overpotential. The final variant (N375C) was found to be less active possibly because of perturbation to the tertiary structure caused by the mutation and/or less efficient coupling to the surface.

The very good stability of the immobilized enzymes allows a detailed study of the kinetics of the electrocatalytic oxygen reduction both for comparison of DET and MET pathways and for systematic studies of the effects of pH and Cl^-. Our studies show that there is a change in the slope of the potential *vs.* pH plot of the electrocatalytic oxygen reduction wave at pH 6.0 from -28 mV to -57 mV per pH unit indicating the influence of an amino acid residue, possibly histidine 463, glutamate 464 or aspartate 107, in the catalytic cycle.

Our work also highlights the effect of Cl^- on the direct oxygen reduction by *Mo*BOD as a function of pH for the immobilized enzyme. We have shown that for the immobilized *Mo*BOD the resting oxidized (RO) form transforms into the alternative resting (AR) state in the presence of

Cl^- and that a more negative potential is required to reduce the AR state and reactivate it for electrocatalysis of oxygen reduction.

AUTHOR INFORMATION

Corresponding Author

* E-mail: p.n.bartlett@soton.ac.uk

ORCID

Philip. N. Bartlett: 0000-0002-7300-6900

Notes

The authors declare no competing financial interest.

ACKNOWLEDGEMENTS

FAA acknowledges financial support from the Ministry of Higher Education and Scientific Research of Iraq. PNB gratefully acknowledges receipt of a Wolfson Research Merit Award. NM thanks the funding of the ANR project BIO3 (ANR-16-CE19-0001-03).

REFERENCES

1. Kjaergaard, C. H.; Durand, F.; Tasca, F.; Qayyum, M. F.; Kauffmann, B.; Gounel, S.; Suraniti, E.; Hodgson, K. O.; Hedman, B.; Mano, N.; Solomon, E. I., Spectroscopic and Crystallographic Characterization of "Alternative Resting" and "Resting Oxidized" Enzyme Forms of Bilirubin Oxidase: Implications for Activity and Electrochemical Behavior of Multicopper Oxidases. *J. Am. Chem. Soc.* **2012,** *134*, 5548-5551.

2. Durand, F.; Gounel, S.; Kjaergaard, C. H.; Solomon, E. I.; Mano, N., Bilirubin Oxidase from *Magnaporthe oryzae*: an Attractive new Enzyme for Biotechnological Applications. *Appl. Microbiol. Biot.* **2012,** *96*, 1489-1498.

3. Mano, N.; de Poulpiquet, A., O_2 Reduction in Enzymatic Biofuel Cells. *Chem. Rev.* **2017,** *118*, 2392-2468.

4. Mano, N.; Kim, H.-H.; Heller, A., On the Relationship between the Characteristics of Bilirubin Oxidases and O_2 Cathodes based on their "Wiring". *J. Phys. Chem. B* **2002,** *106*, 8842-8848.

5. Durand, F.; Kjaergaard, C. H.; Suraniti, E.; Gounel, S.; Hadt, R. G.; Solomon, E. I.; Mano, N., Bilirubin Oxidase from *Bacillus pumilus*: a Promising Enzyme for the

Elaboration of Efficient Cathodes in Biofuel Cells. *Biosens. Bioelectron.* **2012,** *35*, 140-146.

6. Jacquot, C. H.; Lamicq, G.; Salvador, D.; Gounel, S.; Stines-Chaumeil, C.; Mano, N., Bilirubin Oxidase: Enzyme of Choice to Biofuel Cells. *FEBS J* **2014,** *281*, 240-241.

7. Mano, N.; Edembe, L., Bilirubin Oxidases in Bioelectrochemistry: Features and Recent Findings. *Biosens. Bioelectron.* **2013,** *50*, 478-85.

8. Mano, N., Features and Applications of Bilirubin Oxidases. *Appl. Microbiol. Biot.* **2012,** *96*, 301-307.

9. Mizutani, K.; Toyoda, M.; Sagara, K.; Takahashi, N.; Sato, A.; Kamitaka, Y.; Tsujimura, S.; Nakanishi, Y.; Sugiura, T.; Yamaguchi, S.; Kano, K.; Mikami, B., X-ray Analysis of Bilirubin Oxidase from *Myrothecium verrucaria* at 2.3 Angstrom Resolution using a Twinned Crystal. *Acta Cryst. F* **2010,** *66*, 765-770.

10. de Poulpiquet, A.; Kjaergaard, C. H.; Rouhana, J.; Mazurenko, I.; Infossi, P.; Gounel, S.; Gadiou, R.; Giudici-Orticoni, M. T.; Solomon, E. I.; Mano, N.; Lojou, E., Mechanism of Chloride Inhibition of Bilirubin Oxidase and its Dependence on Potential and pH. *ACS Catal.* **2017,** *7*, 3916-3923.

11. Tasca, F.; Farias, D.; Castro, C.; Acuna-Rougier, C.; Antiochia, R., Bilirubin Oxidase from *Myrothecium verrucaria* Physically Absorbed on Graphite Electrodes. Insights into the Alternative Resting Form and the Sources of Activity Loss. *PloS One* **2015,** *10*, e0132181.

12. dos Santos, L.; Climent, V.; Blanford, C. F.; Armstrong, F. A., Mechanistic Studies of the 'Blue' Cu Enzyme, Bilirubin Oxidase, as a Highly Efficient Electrocatalyst for the Oxygen Reduction Reaction. *Phys. Chem. Chem. Phys.* **2010,** *12*, 13962-13974.

13. Xia, H.-Q.; Kitazumi, Y.; Shirai, O.; Kano, K., Enhanced Direct Electron Transfer-Type Bioelectrocatalysis of Bilirubin Oxidase on Negatively Charged Aromatic Compound-Modified Carbon Electrode. *J. Electroanal. Chem.* **2016,** *763*, 104-109.

14. Cracknell, J. A.; McNamara, T. P.; Lowe, E. D.; Blanford, C. F., Bilirubin Oxidase from *Myrothecium verrucaria*: X-ray Determination of the Complete Crystal Structure and a Rational Surface Modification for Enhanced Electrocatalytic O_2 Reduction. *Dalton Trans.* **2011,** *40*, 6668-6675.

15. Jonsson-Niedziolka, M.; Kaminska, A.; Opallo, M., Pyrene-Functionalised Single-Walled Carbon Nanotubes for Mediatorless Dioxygen Bioelectrocatalysis. *Electrochim. Acta* **2010,** *55*, 8744-8750.

16. Liu, W.; Wang, L.; Jiang, R., Specific Enzyme Immobilization Approaches and their Application with Nanomaterials. *Top. Catal.* **2012,** *55*, 1146-1156.

17. Al-Lolage, F. A.; Meneghello, M.; Ma, S.; Ludwig, R.; Bartlett, P. N., A Flexible Method for the Stable, Covalent Immobilization of Enzymes at Electrode Surfaces. *ChemElectroChem* **2017,** *4*, 1528-1534.

18. Wright, E. J.; Sosna, M.; Bloodworth, S.; Kilburn, J. D.; Bartlett, P. N., Design of Maleimide-Functionalised Electrodes for Covalent Attachment of Proteins Through Free Surface Cysteine Groups. *Chem. Eur. J.* **2014,** *20*, 5550-5554.

19. Bartlett, P. N.; Al-Lolage, F. A., There is no Evidence to Support Literature Claims of Direct Electron Transfer (DET) for Native Glucose Oxidase (GOx) at Carbon Nanotubes or Graphene. *J. Electroanal. Chem.* **2018,** *819*, 26-37.

20. Groppi, J.; Bartlett, P. N.; Kilburn, J. D., Toward the Control of the Creation of Mixed Monolayers on Glassy Carbon Surfaces by Amine Oxidation. *Chem. Eur. J.* **2016,** *22*, 1030-1036.

21. Pita, M.; Gutierrez-Sanchez, C.; Toscano, M. D.; Shleev, S.; De Lacey, A. L., Oxygen Biosensor Based on Bilirubin Oxidase Immobilized on a Nanostructured Gold Electrode. *Bioelectrochem.* **2013,** *94*, 69-74.

22. Lalaoui, N.; Holzinger, M.; Le Goff, A.; Cosnier, S., Diazonium Functionalisation of Carbon Nanotubes for Specific Orientation of Multicopper Oxidases: Controlling Electron Entry Points and Oxygen Diffusion to the Enzyme. *Chem. Eur. J.* **2016,** *22*, 10494-10500.

23. Lee, S.; Zhang, Z.; Wang, X.; Pfefferle, L. D.; Haller, G. L., Characterization of Multi-Walled Carbon Nanotubes Catalyst Supports by Point of Zero Charge. *Catal. Today* **2011,** *164*, 68-73.

24. Mazurenko, I.; Monsalve, K.; Rouhana, J.; Parent, P.; Laffon, C.; Le Goff, A.; Szunerits, S.; Boukherroub, R.; Giudici-Orticoni, M.-T.; Mano, N.; Lojou, E., How the Intricate Interactions between Carbon Nanotubes and Two Bilirubin Oxidases Control Direct and Mediated O_2 Reduction. *ACS Appl. Mater. Interfaces* **2018,** *8*, 23074−23085.

25. Yang, S.; Liu, J.; Quan, X.; Zhou, J., Bilirubin Oxidase Adsorption onto Charged Self-Assembled Monolayers: Insights from Multiscale Simulations. *Langmuir* **2018,** *34*, 9818-9828.

26. Leger, C.; Jones, A. K.; Albracht, S. P. J.; Armstrong, F. A., Effect of a Dispersion of Interfacial Electron Transfer Rates on Steady State Catalytic Electron Transport in NiFe -Hydrogenase and other Enzymes. *J. Phys. Chem. B* **2002,** *106*, 13058-13063.

27. Leger, C.; Heffron, K.; Pershad, H. R.; Maklashina, E.; Luna-Chavez, C.; Cecchini, G.; Ackrell, B. A. C.; Armstrong, F. A., Enzyme Electrokinetics: Energetics of Succinate Oxidation by Fumarate Reductase and Succinate Dehydrogenase. *Biochem.* **2001,** *40*, 11234-11245.

28. Jones, A. K.; Sillery, E.; Albracht, S. P. J.; Armstrong, F. A., Direct Comparison of the Electrocatalytic Oxidation of Hydrogen by an Enzyme and a Platinum Catalyst. *Chem. Commun.* **2002**, 866-867.

29. Butt, J. N.; Thornton, J.; Richardson, D. J.; Dobbin, P. S., Voltammetry of a Flavocytochrome c(3): the Lowest Potential Heme Modulates Fumarate Reduction Rates. *Biophys. J.* **2000,** *78*, 1001-1009.

30. Hirst, J.; Sucheta, A.; Ackrell, B. A. C.; Armstrong, F. A., Electrocatalytic Voltammetry of Succinate Dehydrogenase: Direct Quantification of the Catalytic

Properties of a Complex Electron-Transport Enzyme. *J. Am. Chem. Soc.* **1996,** *118*, 5031-5038.

31. Bateman, L.; Leger, C.; Goodin, D. B.; Armstrong, F. A., A Distal Histidine Mutant (H52Q) of Yeast Cytochrome c Peroxidase Catalyzes the Oxidation of H_2O_2 instead of its Reduction. *J. Am. Chem. Soc.* **2001,** *123*, 9260-9263.

32. Lalaoui, N.; Le Goff, A.; Holzinger, M.; Cosnier, S., Fully Oriented Bilirubin Oxidase on Porphyrin-Functionalized Carbon Nanotube Electrodes for Electrocatalytic Oxygen Reduction. *Chem. Eur. J.* **2015,** *21*, 16868-16873.

33. Frew, J. E.; Hill, H. A. O., Direct and Indirect Electron-Transfer between Electrodes and Redox Proteins. *Eur. J. Biochem.* **1988,** *172*, 261-269.

34. Gutierrez-Sanchez, C.; Ciaccafava, A.; Blanchard, P. Y.; Monsalve, K.; Giudici-Orticoni, M. T.; Lecomte, S.; Lojou, E., Efficiency of Enzymatic O_2 Reduction by *Myrothecium verrucaria* Bilirubin Oxidase Probed by Surface Plasmon Resonance, PMIRRAS, and Electrochemistry. *ACS Catal.* **2016,** *6*, 5482-5492.

35. Kamitaka, Y.; Tsujimura, S.; Ikeda, T.; Kano, K., Electrochemical Quartz Crystal Microbalance Study of Direct Bioelectrocatalytic Reduction of Bilirubin Oxidase. *Electrochem.* **2006,** *74*, 642-644.

36. Singh, K.; McArdle, T.; Sullivan, P. R.; Blanford, C. F., Sources of Activity Loss in the Fuel Cell Enzyme Bilirubin Oxidase. *Energy Environ. Sci.* **2013,** *6*, 2460-2464.

37. Zheng, W.; Zhao, H. Y.; Zhou, H. M.; Xu, X. X.; Ding, M. H.; Zheng, Y. F., Electrochemistry of Bilirubin Oxidase at Carbon Nanotubes. *J. Solid State Electr.* **2009,** *14*, 249-254.

38. Ramirez, P.; Mano, N.; Andreu, R.; Ruzgas, T.; Heller, A.; Gorton, L.; Shleev, S., Direct Electron Transfer from Graphite and Functionalized Gold Electrodes to T1 and T2/T3 Copper Centers of Bilirubin Oxidase. *BBA-Bioenergetics* **2008,** *1777*, 1364-1369.

39. Christenson, A.; Shleev, S.; Mano, N.; Heller, A.; Gorton, L., Redox Potentials of the Blue Copper Sites of Bilirubin Oxidases. *BBA-Bioenergetics* **2006,** *1757*, 1634-1641.

40. Ivnitski, D.; Artyushkova, K.; Atanassov, P., Surface Characterization and Direct Electrochemistry of Redox Copper Centers of Bilirubin Oxidase from Fungi *Myrothecium verrucaria*. *Bioelectrochem.* **2008,** *74*, 101-110.

41. Brocato, S.; Lau, C.; Atanassov, P., Mechanistic Study of Direct Electron Transfer in Bilirubin Oxidase. *Electrochim. Acta* **2012,** *61*, 44-49.

42. Shleev, S.; Tkac, J.; Christenson, A.; Ruzgas, T.; Yaropolov, A. I.; Whittaker, J. W.; Gorton, L., Direct Electron Transfer between Copper-Containing Proteins and Electrodes. *Biosens. Bioelectron.* **2005,** *20*, 2517-2554.

43. Ivnitski, D. M.; Khripin, C.; Luckarift, H. R.; Johnson, G. R.; Atanassov, P., Surface Characterization and Direct Bioelectrocatalysis of Multicopper Oxidases. *Electrochim. Acta* **2010,** *55*, 7385-7393.

44. Shleev, S.; Jarosz-Wilkolazka, A.; Khalunina, A.; Morozova, O.; Yaropolov, A.; Ruzgas, T.; Gorton, L., Direct Electron Transfer Reactions of Laccases from Different Origins on Carbon Electrodes. *Bioelectrochem.* **2005,** *67*, 115 - 124.

45. Shleev, S.; Andoralov, V.; Falk, M.; Reimann, C. T.; Ruzgas, T.; Srnec, M.; Ryde, U.; Rulisek, L., On the Possibility of Uphill Intramolecular Electron Transfer in Multicopper Oxidases: Electrochemical and Quantum Chemical Study of Bilirubin Oxidase. *Electroanal.* **2012,** *24*, 1524-1540.

46. Filip, J.; Tkac, J., The pH Dependence of the Cathodic Peak Potential of the Active Sites in Bilirubin Oxidase. *Bioelectrochem.* **2014,** *96*, 14-20.

47. Weigel, M. C.; Tritscher, E.; Lisdat, F., Direct Electrochemical Conversion of Bilirubin Oxidase at Carbon Nanotube-Modified Glassy Carbon Electrodes. *Electrochem. Commun.* **2007,** *9*, 689-693.

48. Jeuken, L. J. C.; Wisson, L. J.; Armstrong, F. A., The Kinetics of a Weakly Electron-Coupled Proton Transfer in Azurin. *Inorg. Chim. Acta* **2002,** *331*, 216-223.

49. Miura, Y.; Tsujimura, S.; Kurose, S.; Kamitaka, Y.; Kataoka, K.; Sakurai, T.; Kano, K., Direct Electrochemistry of CueO and its Mutants at Residues to and near Type I Cu for Oxygen-Reducing Biocathode. *Fuel Cells* **2009,** *9*, 70-78.

50. Bento, I.; Silva, C. S.; Chen, Z.; Martins, L. O.; Lindley, P. F.; Soares, C. M., Mechanisms Underlying Dioxygen Reduction in Laccases. Structural and Modelling Studies Focusing on Proton Transfer. *BMC Struct. Biol.* **2010,** *10*, 28-42.

51. Iwaki, M.; Kataoka, K.; Kajino, T.; Sugiyama, R.; Morishita, H.; Sakurai, T., ATR-FTIR Study of the Protonation States of the Glu Residue in the Multicopper Oxidases, CueO and Bilirubin Oxidase. *FEBS Lett.* **2010,** *584*, 4027-4031.

52. Silva, C. S.; Damas, J. M.; Chen, Z.; Brissos, V.; Martins, L. O.; Soares, C. M.; Lindley, P. F.; Bento, I., The Role of Asp116 in the Reductive Cleavage of Dioxygen to Water in CotA Laccase: Assistance during the Proton-Transfer Mechanism. *Acta Crys. D* **2012,** *68*, 186-193.

53. Quintanar, L.; Stoj, C.; Wang, T. P.; Kosman, D. J.; Solomon, E. I., Role of Aspartate 94 in the Decay of the Peroxide Intermediate in the Multicopper Oxidase Fet3p. *Biochem.* **2005,** *44*, 6081-6091.

54. Brissos, V., Chen, Z., & Martins, L. O., The Kinetic Role of Carboxylate Residues in the Proximity of the Trinuclear Centre in the O_2 Reactivity of CotA-Laccase. *Dalton Trans.* **2012,** *41* 6247-6255.

55. Chen, Z.; Durao, P.; Silva, C. S.; Pereira, M. M.; Todorovic, S.; Hildebrandt, P.; Bento, I.; Lindley, P. F.; Martins, L. O., The Role of Glu(498) in the Dioxygen Reactivity of CotA-Laccase from *Bacillus subtilis*. *Dalton Trans.* **2010,** *39*, 2875-2882.

56. Hirose, J.; Inoue, K.; Sakuragi, H.; Kikkawa, M.; Minakami, M.; Morikawa, T.; Iwamoto, H.; Hiromi, K., Anions Binding to Bilirubin Oxidase from *Trachyderma tsunodae* K-2593. *Inorg. Chim. Acta* **1998,** *273*, 204-212.

57. Kjaergaard, C. H.; Jones, S. M.; Gounel, S.; Mano, N.; Solomon, E. I., Two-Electron Reduction versus One-Electron Oxidation of the Type 3 Pair in the Multicopper Oxidases. *J. Am. Chem. Soc.* **2015,** *137*, 8783-94.

58. Solomon, E. I.; Augustine, A. J.; Yoon, J., O_2 Reduction to H_2O by the Multicopper Oxidases. *Dalton Trans.* **2008,** *37*, 3921-3932.